

# Determination of copy number variations and affected gene networks in breast cancer

VIOLETA LARIOS-SERRATO<sup>1\*</sup>, HILDA-ALICIA VALDEZ-SALAZAR<sup>2\*</sup>, JAVIER TORRES<sup>2</sup>,  
MARGARITA CAMORLINGA-PONCE<sup>2</sup>, PATRICIA PIÑA-SÁNCHEZ<sup>3</sup>,  
HÉCTOR MAYANI<sup>3</sup> and MARTHA-EUGENIA RUIZ-TACHIQUÍN<sup>3</sup>

<sup>1</sup>Laboratory of Biotechnology and Genomic Bioinformatics, National School of Biological Sciences,  
National Polytechnic Institute, Lázaro Cárdenas Professional Unit, Mexico City 11340, Mexico;

<sup>2</sup>Infectious and Parasitic Diseases Medical Research Unit, High Specialty Medical Unit-Pediatrics Hospital  
'Dr Silvestre Frenk Freund', XXI Century National Medical Center, Mexican Social Security Institute,  
Mexico City 06720, Mexico; <sup>3</sup>Oncological Diseases Medical Research Unit, High Specialty Medical Unit-Oncology  
Hospital, XXI Century National Medical Center, Mexican Social Security Institute, Mexico City 06720, Mexico

Received October 2, 2025; Accepted February 26, 2026

DOI: 10.3892/br.2026.2158

**Abstract.** Triple-negative breast cancer (TNBC) is a highly aggressive form characterized by limited therapeutic options and notable molecular diversity. The present study performed a genome-wide analysis of copy number variations (CNVs) using high-density microarrays in tumor tissue (TUM), adjacent non-tumor tissue (ADJ) and leukocytes (LEU) obtained from five patients with TNBC. The present study identified both unique and shared CNVs across tissue samples, including alterations in key chromosomal regions such as 1q23.3, 1q32.1 and 8q24.3, which harbor oncogenes such as MYC, myeloid cell leukemia 1 (MCL1) and BCL9. Losses in 6q25.2 affecting estrogen receptor 1 (ESR1) gene were also detected. CNVs were enriched in genes associated with Hallmarks of Cancer, with TUM samples showing profiles associated with 'proliferation', 'metastasis' and 'immune evasion', ADJ samples with 'growth suppression' and LEU samples with 'genomic instability'. Pathway enrichment analyses revealed disrupted functions in 'DNA repair', 'extracellular matrix organization' and 'TP53 signaling' in TUM. Notably, EGFR, excision repair cross-complementing group 4 (ERCC4) and heat shock protein 90 alpha family class B

member 1 (HSP90AB1) genes emerged as potential central nodes in interaction networks and may serve as markers or therapeutic targets. To the best of our knowledge, the present study is the first CNV profiling study in TNBC in Mexican patients, highlighting the importance of including underrepresented populations in genomic research to uncover distinct molecular signatures and potential diagnostic or therapeutic avenues. Bioinformatically predicted molecular signatures of TNBC involve both common and distinct CNV-associated Hallmarks of Cancer genes, which represent candidates for screening as potential TNBC biomarkers.

## Introduction

Despite advances in understanding of cancer biology, breast cancer (BC) has the highest incidence (2,296,840 new cases) and mortality (666,103 deaths) in female patients worldwide (1).

Cancer is a group of genetic diseases, highlighting the need to identify biomarkers for its prevention, diagnosis, treatment response prediction and survival estimation. The present study focused on the analysis of copy number variations (CNVs), the changes in the number of copies of DNA sequences within a genome. CNVs include insertions, deletions and duplications of DNA segments and explain a notable proportion of the genetic variability between healthy individuals and patients with cancer. The analysis of genomic alterations in BC patients worldwide has led to the identification of gene sets characterized by CNVs, including both losses and gains, which are grouped into specific molecular signatures or profiles. These profiles are integrated into interaction networks that align with the Hallmarks of Cancer (2). This approach aims to identify new marker molecules for neoplasia in the different molecular subtypes.

BC is the most common malignancy among female patients in developed countries, with genetic susceptibility playing a notable contributory role. Despite extensive research, a notable proportion of hereditary BC predisposition remains

---

*Correspondence to:* Dr Martha-Eugenia Ruiz-Tachiquín, Oncological Diseases Medical Research Unit, High Specialty Medical Unit-Oncology Hospital, XXI Century National Medical Center, Mexican Social Security Institute, 330 Cuauhtémoc Avenue, Colonia Doctores, Alcaldía Cuauhtémoc, Mexico City 06720, Mexico  
E-mail: mertachiquin@gmail.com

\*Contributed equally

**Key words:** CNV, gene, interaction network, breast cancer, high-density array

unexplained, indicating the need for further exploration of genetic variations (3-6).

Studies have identified CNVs as prevalent structural variations in the human genome, contributing to the risk of developing BC (7,8). CNVs involve alterations in the number of copies of specific DNA segments and range from small alterations to notable chromosomal changes. While small CNVs are typically benign, larger ones are associated with severe consequences such as developmental disorders and cancer (9). High-resolution genome-wide scans have demonstrated that patients with BC show a higher frequency of rare CNVs compared with healthy controls, suggesting that these variations serve a critical role in hereditary BC risk (10,11). The complexity of BC is further highlighted by its molecular heterogeneity; BC is categorized into subtypes based on specific genetic and phenotypic features (7). These subtypes include luminal A and B, HER2-positive and basal-like types, each defined by distinct receptor profiles and treatment responses (7). Notably, CNVs associated with these subtypes influence gene expression, molecular subtyping and personalized treatment strategies, emphasizing the importance of understanding CNVs in BC (9). CNV profiles may serve as effective biomarkers for BC diagnosis and prognosis (9). In Latin America, founder mutations have been identified, highlighting the ethnic diversity in genetic variations affecting BC risk (12). Understanding these variations and their associated gene networks in patients is key for developing targeted therapies and improving clinical outcomes.

The present study focused on samples from patients lacking hormonal receptors and HER2 expression, specifically those diagnosed with triple-negative breast cancer (TNBC), a subtype characterized by limited treatment options and increased tumor aggressiveness. With the aim of contributing to personalized and precision medicine approaches, the present study analyzed tumor (TUM) and adjacent non-tumor tissue (ADJ) and peripheral blood [leukocytes (LEU)] from each patient.

## Materials and methods

**Samples.** The present study examined samples from five adult females (designated CM09, CM10, CM27, CM30 and CM64) with a median age of 61.5 years and an age range of 35-88 years. A total of two pathologists independently assessed the histopathological features of these specimens.

Participants were recruited from April 2010 to May 2013 from the Oncology Hospital of the XXI Century National Medical Center (Mexico City, Mexico). Inclusion criteria were as follows: Adult female patients with a confirmed histopathological diagnosis of TNBC, adequate tumor cell content ( $\geq 70\%$  neoplastic cells in the biopsy), and availability of tumor, adjacent non-tumor and peripheral blood samples with sufficient DNA concentration and purity for downstream analyses. Exclusion criteria included the absence of a confirmed TNBC diagnosis, diagnosis of other malignancy or cases of cancer recurrence. Samples with insufficient DNA concentration or purity for downstream analyses were also excluded. A total of 14 samples were analyzed, comprising TUM (n=5), ADJ (distance, 1 cm; n=5) and peripheral blood

(LEU, n=4). Histological assessment of the biopsies was performed by two trained pathologists independently. They assigned the phenotypic diagnosis of TNBC. Only biopsy samples for which both pathologists independently reached the same TNBC diagnosis were included in the study.

The present study was approved (approval no. 2008-785-001) by the Scientific and Ethics Committees of Health Research Coordination of Mexican Social Security Institute, Mexico City, Mexico. All participants were informed about the nature of the study and provided written informed consent. The study was conducted in accordance with best clinical practice and all participant identities were anonymized. Immunohistochemistry data were obtained from the pathology and clinical records of the patients. All samples were TNBC.

**DNA extraction.** DNA was extracted from TUM, ADJ and LEU using a commercial kit (QIAamp<sup>®</sup> Micro kit, cat. no. 56304, Qiagen GmbH) as previously described (13). Samples were digested with proteinase K for 3 days at 56°C in a water bath, with fresh enzyme added every 24 h.

**DNA quality assessment and preparation.** The extracted DNA was quantified by spectrophotometry using a Nanodrop 2000 instrument (Thermo Fisher Scientific, Inc.). DNA quality was assessed by Multiplex PCR (Multiplex PCR kit, Qiagen GmbH) employing primers designed to amplify different regions of GAPDH gene as previously described (14). PCR amplification was performed as follows: Initial denaturation at 95°C for 15 min, followed by 40 cycles of 94°C for 30 sec, 57°C for 90 sec, and 72°C for 90 sec and final extension at 72°C for 10 min. PCR products were visualized by electrophoresis on a 2% agarose gel, stained with RedGel<sup>®</sup> Nucleic Acid Gel Stain (Biotium, Inc.) and documented using an ultraviolet transilluminator system (Syngene). The dye was placed in the molten agarose during gel preparation.

**High-density whole-genome microarray analysis.** Samples were analyzed using Affymetrix<sup>®</sup> CytoScan<sup>™</sup> microarrays according to the manufacturer's protocol, starting with 250 ng DNA. An additional five PCR cycles were included to increase DNA yield. PCR products (90  $\mu$ g) were fragmented and labeled through an additional PCR labeling step using the Cytoscan<sup>™</sup> HD Suite which included Cytoscan HD matrices and Cytoscan reagent kit (cat. no. 901835); Thermo Fisher Scientific, Inc.

**CNV processing.** Raw intensity files (.CEL) obtained from the Affymetrix<sup>®</sup> CytoScan<sup>™</sup> HD Array platform (Thermo Fisher Scientific, Inc.) (13) were analyzed using the proprietary Chromosome Analysis Suite (ChAS) software (version 4.3.0.71; Thermo Fisher Scientific, Inc.). The CytoScanHD\_Array.na36.annot.db file was employed for annotation, with the GRCh38 (February 2013) human genome assembly (Genome Reference Consortium, 2013; [https://www.ncbi.nlm.nih.gov/assembly/GCF\\_000001405.26/](https://www.ncbi.nlm.nih.gov/assembly/GCF_000001405.26/)) serving as the reference model.

Data processing was performed using the Circular Binary Segmentation algorithm embedded in ChAS software (version 4.3.0.71; Thermo Fisher Scientific, Inc.) (15), in which the Log<sub>2</sub> ratio for each marker was calculated relative

to the reference signal profile. CNV analysis was performed following normalization to baseline reference intensities based on the Chromosome Analysis Suite (ChAS) software (version 4.3.0.71; Thermo Fisher Scientific, Inc.) reference model, which included 284 HapMap samples and 96 healthy control individuals (15). The hidden Markov model (16) implemented in ChAS software (version 4.3.0.71; Thermo Fisher Scientific, Inc.) was applied to determine CN-state and corresponding breakpoints.

A customized high-resolution filter was applied for detection of CNVs, defining CN-gains as regions containing  $\geq 50$  markers and  $\geq 400$  kbp and CN-losses as regions containing  $\geq 50$  markers and  $\geq 100$  kbp. Quality control was performed using the median absolute pairwise difference (MAPD) and single nucleotide polymorphism-quality control (SNP-QC) score. Only samples with MAPD  $< 0.25$  and SNP-QC  $> 15$  were included in the subsequent analyses. Other parameters were as follows: Gene coverage  $> 36,000$  RefSeq genes with one marker/880 bases; backbone (non-gene) coverage of one marker/1,737 bases; highest density of SNPs and CN-probes for whole-genome coverage; 2.67 million markers; 750,000 SNPs; 1.9 million non-polymorphic probes; enriched gene coverage for cancer and germline or inherited genetic variation; X chromosome genes (one marker/486 bases); covering 12,000 Online Mendelian Inheritance in Man (OMIM) genes (one marker/659 bases); cancer gene coverage (one marker/553 bases); CN-resolution  $< 25$  kb; 99.9% sensitivity.

**Bioinformatic analysis.** A custom Perl script was developed to process the CNV segment data files generated by ChAS software (version 4.3.0.71; Thermo Fisher Scientific, Inc.) for each sample. The script compared all individual CNV files to compile a comprehensive gene table including the frequency of affected patients, CNV event type (gain or loss), chromosomal position, cytogenetic band and gene function, disease associations and inheritance patterns retrieved from the OMIM database (omim.org) (17). Additional annotations were integrated from Haploinsufficiency Prediction version 3 from the DECIPHER database v11.35 (deciphergenomics.org) (18), and gene information from dbEMT 2.0 (dbemt.bioinfo-minzhao.org) (18,19).

Genes altered in  $\geq 3$  patients with TNBC were included for further analysis and visualization. In the absence of an established measurement (gold standard), an arbitrary value was determined to provide guidance in exploring relevant alterations. The present study analyzed CNV type (gain or loss), chromosomal location, cytoband, cumulative length, number of affected patients, associated genes, haploinsufficiency scores, EMT-gene status and disease associations associated with CNVs of TUM, ADJ and LEU. Genes altered in  $\geq 3$  in TUM, ADJ and LEU samples were included for analysis and visualization. A karyotype was generated (Fig. 1), using the KaryoploteR package (version 1.30.0; bioconductor.org/packages/karyoploteR/) (20) in combination with biomaRt (version 2.60.1; bioconductor.org/packages/biomaRt/) (21). Gene overlap analysis was conducted by generating Venn diagrams using the Jvenn web server (22). Hallmarks of Cancer enrichment analysis (adjusted  $P < 0.05$ ) was performed using 6,763 genes (23) (Fig. 2).

Metabolic pathway enrichment analysis was performed with Reactome (version 88) (24), considering results with a false discovery rate (FDR)  $< 0.05$  as statistically significant. To identify the Hallmarks of Cancer associated with the TUM, ADJ and LEU profiles, an interaction network was constructed by CNV types (gains and losses), integrating genetic and physical interactions, biological pathways and predicted associations (Fig. 3). Network generation and visualization were performed using STRING (25), GeneMANIA (26) and Cytoscape (version 3.10.3) (27). Network connections were established based on direct interactions, shared neighbors and weight scores to identify the most significant gene associations. Manual annotation of the corresponding Hallmarks of Cancer, including 'adhesion', 'angiogenesis', 'inflammation', 'migration', 'metastasis', 'morphogenesis', 'proliferation' and 'survival' (2) was performed using databases including The Human Protein Atlas (28), the NCBI Gene database (ncbi.nlm.nih.gov/gene/), UniProt (<https://www.uniprot.org/>) and GeneCards (genecards.org/).

CNV profiles identified in TUM, ADJ and LEU samples were compared against publicly available copy number data from The Cancer Genome Atlas [(TCGA) TNBC cohort ( $n=139$ ), accessed through cBioPortal (cbioportal.org), TCGA dataset accession: TCGA-BRCA; study ID: brca\_tcga; (29); Cancer Genome Atlas Network, 2012 (30)], to identify shared and potentially population-specific chromosomal alterations.

**Statistical analysis.** CNV data are presented as categorical genomic events (gains or losses) with associated genomic coordinates, affected genes and frequency across patients (cut-off,  $\geq 3$  patients). Data are summarized by frequency counts, cumulative genomic lengths (cl) in megabase pairs (Mbp) and enrichment statistics.  $P < 0.05$  was considered to indicate a statistically significant difference. Enrichment significance was evaluated using Fisher's exact test with Benjamini-Hochberg correction for multiple comparisons. Pathway enrichment analyses were performed in Reactome (v.88) and the Hallmarks of Cancer tool (23,24), both of which apply hypergeometric testing with FDR correction. Data analysis was performed using R software (version 4.4.0; R-project.org) and the RStudio environment (version 2025.05.0+496; Posit PBC; posit.co), incorporating packages from Bioconductor (version 3.21; bioconductor.org): KaryoploteR (v1.30.0; bioconductor.org/packages/karyoploteR), biomaRt (v2.60.1; bioconductor.org/packages/biomaRt), ReactomePA (v1.50.0; bioconductor.org/packages/ReactomePA) (31) for pathway enrichment, and ggplot2 (v3.5.1; cran.r-project.org/web/packages/ggplot2) (32) for data visualization.

## Results

**Sample characteristics.** Samples were collected from five patients with TNBC (third-generation Mexicans), aged 35–88 years, including four treatment-naïve individuals and one patient who had received prior therapy (Table I). Four samples corresponded to infiltrating ductal carcinoma (IDC) and one to lobular carcinoma (LC; Table I). The proportion of neoplastic cells in the tumor tissues ranged from 70 to 100%. The present study analyzed samples from five female patients diagnosed with TNBC, including both IDC and LC.

Table I. Patient and sample characteristics.

ID	Sample type	Cancer type	Sex	Age, years	TNM stage	Clinical stage	Prior treatment	Tumor cell proportion, %
CM09	LEU, ADJ, TUM	IDC	F	80	T2N0M0	IIA	None	95
CM10	LEU, ADJ, TUM	IDC	F	35	T2N2M0	IIIA	None	100
CM27	LEU, ADJ, TUM	LC	F	88	T2N1M0	IIB	None	80
CM30	LEU, ADJ, TUM	IDC	F	64	NA	NA	None	70
CM64	ADJ, TUM	IDC	F	61	T2N0M0	IIA	With	70

LEU, leukocytes; ADJ, adjacent non-tumor tissue; TUM, tumor tissue; IDC, infiltrating ductal carcinoma; LC, lobular carcinoma; F, female; NA, not applicable.

Table II. Immunohistochemistry data.

ID	ER	PR	HER2	Ki67	CK5
CM09	Negative	Negative	Negative	Negative	Positive
CM10	Negative	Negative	Negative	Negative	Negative
CM27	Negative	Negative	Negative	Positive	Negative
CM30	Negative	Negative	Negative	Negative	Negative
CM64	Negative	Negative	Negative	Positive	Positive

ER, estrogen receptor; PR, progesterone receptor; HER2, human epidermal growth factor receptor 2; Ki67, marker of proliferation Ki-67; CK5, cytokeratin 5.

Clinical staging was T2N0M0 (stage IIA) for CM09 and CM64, T2N2M0 (stage IIIA) for CM10, T2N1M0 (stage IIB) for CM27; data was not available for CM30. All patients were treatment-naïve at the time of sample collection, except CM64, whose prior treatment records were unavailable.

The immunohistochemical analysis of the samples revealed a heterogeneous profile of biomarkers (Table II). All five cases were negative for HER2, estrogen receptor (ER) and progesterone receptor (PR) expression. Ki67 expression was positive in CM27 and CM64, suggesting a higher proliferative index in these tumors. CK5 was positive in two cases (CM09 and CM64), indicating a possible basal phenotype. Overall, the cohort displayed a predominance of TNBC features, with variability in proliferation and basal markers.

*Genomic detection of CNVs.* The CNVs were estimated based on regions where the majority of SNPs do not exhibit heterozygosity. Table III summarizes the chromosomes with the highest frequency of CNV events, reflecting recurrent alterations, although exact chromosomal coordinates were not identical across samples.

To identify the most relevant CNVs in TNBC, alterations detected in  $\geq 3$  patients were analyzed. A similar distribution pattern was observed across all CNVs, with the highest number of events detected in tumor (TUM) samples ( $n=1,717$ ), followed by adjacent non-tumor tissue (ADJ;  $n=132$ ) and leukocytes (LEU;  $n=13$ ) samples (Table SI). In addition, Table SII presents the accumulated CNV length per chromosome to assess whether larger losses were associated with increased genomic disruption.

In TUM samples, the chromosomes most affected based on cumulative CNV length (Mbp-cl) and the number of CNV events were chromosome 3 (gains) and chromosome 5 (losses). In ADJ samples, chromosomes 8 (gains) and 4 (losses) were predominantly altered, whereas in LEU samples, chromosome 4 exhibited both gains and losses (Table SII). Notably, in TUM and ADJ samples, the most frequent CNV sizes ranged from 200 to 500 kbp for gains and from 100 to 200 kbp for losses (Table SIII).

In TUM, recurrent gains were observed in 1q23.3 (12.77 Mbp-cl) and 1q32.1 (7.03 Mbp-cl), as well as in the 8q24.22-8q24.3 region (20.32 and 16.25 Mbp-cl, respectively), while a loss was noted in 6q25.2 (3.18 Mbp-cl; Table SIV). ADJ displayed gains in cytobands 1p36.32, 4p16.1, 5p15.33, 8q24.3 and 20q13.33 (Table SIV). LEU presented both gains and losses, including a loss at 8p11.22 and 14q11.2 and gains at 14q32.33 and 22q11.22 (Table SIV). The total number of gains and losses per chromosome across all three tissue types is summarized in Tables SII and IV.

These findings indicate that CNVs were not restricted to TUM samples but also present in ADJ and LEU, potentially reflecting early or systemic genomic instability. Such alterations may serve as potential biomarkers and provide insight into the interactions between the tumor and its microenvironment.

*BC genes are associated with CNVs.* A Venn diagram was constructed to examine CNV-TNBC-relevant genes present in  $\geq 3$  patients across TUM, ADJ and LEU samples (Fig. 2A). The present study identified 1,615 CNV unique genes in

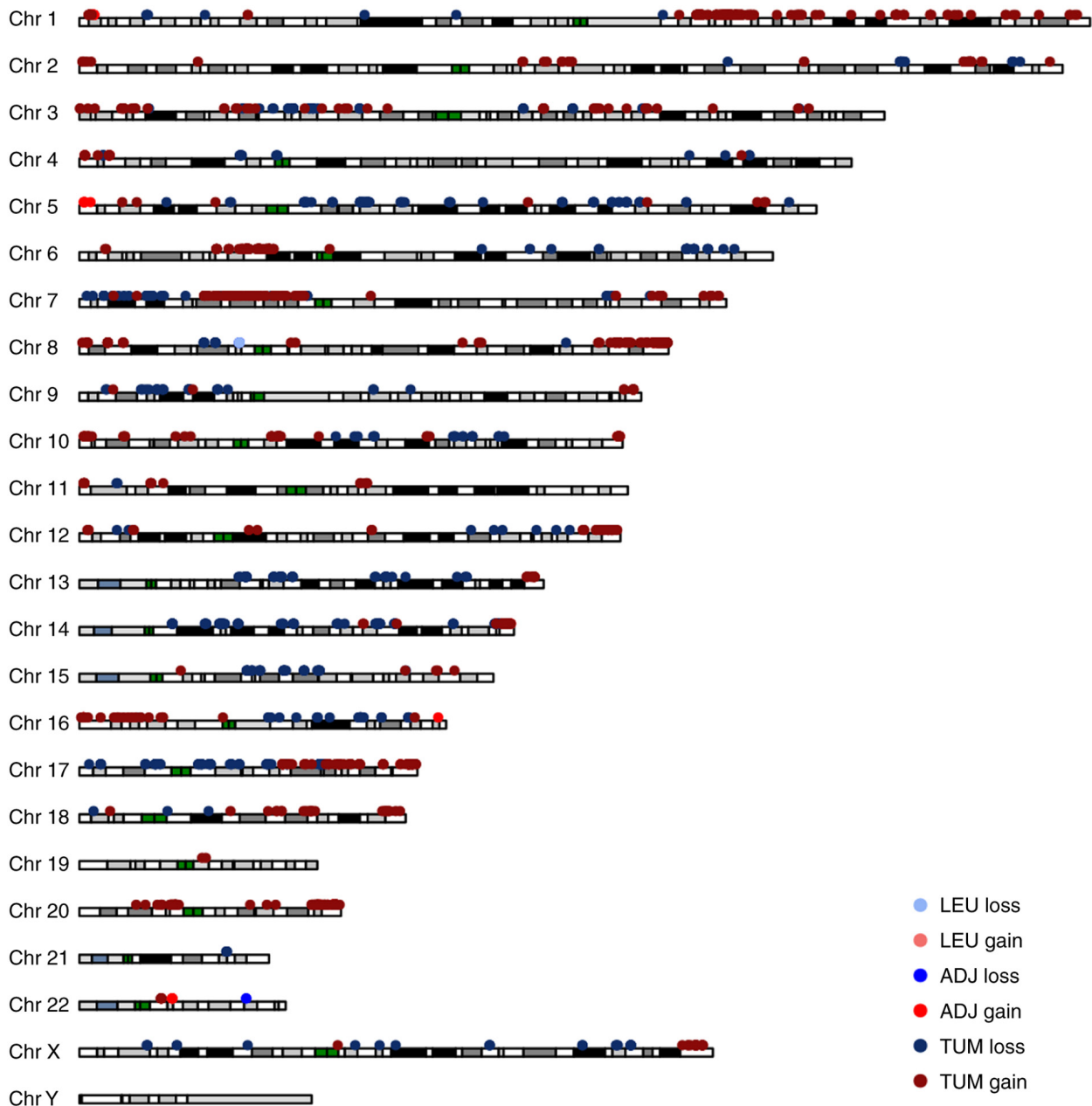


Figure 1. Karyogram showing distribution of CNVs in triple negative breast cancer samples. CNV events across Chr 1-22, X and Y in  $\geq 3$  samples. CNVs, copy number variations; TUM, tumor tissue; ADJ, adjacent non-tumor tissue; LEU, leukocytes; Chr, chromosome.

TUM, 25 in ADJ and one in LEU (Fig. 2; Table SV). Of the 95 genes shared between TUM and ADJ, six carried Hallmarks of Cancer annotations [ADGRB1, CHRNA4, RecQ-like helicase (RECQL)4, SSTR5, TONSL and UVSSA; Table SV], suggesting functional relevance across both tissue compartments. These six shared genes exhibited a greater number of enriched hallmarks compared with LEU (Fig. 2B-D).

The genes altered in TUM were associated with ‘sustaining proliferative signaling’, ‘tumor-promoting inflammation’, ‘tissue invasion and metastasis’, ‘evading immune destruction’, ‘resisting cell death’, ‘evading growth suppressors’ and ‘reprogramming energy metabolism’. In ADJ, altered genes were linked to ‘evading growth suppressors’. In LEU, the single altered gene (IGLL5) was annotated with ‘genome instability’

as a Hallmarks of Cancer category (Fig. 2); however, no statistically significant pathway enrichment was identified in this sample type (Table V).

Comparison with TCGA-TNBC data (Table SVI) revealed both shared and potentially population-specific patterns. Alterations in 8q24.3 (MYC amplification) were common in both the present study cohort and the TCGA-TNBC cohort, consistent with this being a canonical TNBC alteration (29,30). However, the present study observed a higher frequency of gains in 1q23.3 and losses in 6q25.2, although the small sample size ( $n=5$ ) precluded statistical testing of these differences (30,33).

*Functional pathway analysis.* Metabolic pathways were predicted in Reactome using *Homo sapiens* as the model

Table III. Chromosomes with copy number variations and cl in TUM, ADJ and LEU samples.

A, TUM				
Chromosome	Number of events		Mbp-cl	
	Gain	Loss	Gain	Loss
1	77	3	64.82	2.38
3	129	8	71.16	3.41
5	16	32	21.52	97.18
7	35	23	56.93	27.07
13	1	18	12.85	64.94

B, ADJ				
Chromosome	Number of events		Mbp-cl	
	Gain	Loss	Gain	Loss
1	10	0	3.87	0.00
2	2	0	4.75	0.00
4	4	1	1.19	0.42
8	19	0	9.04	0.00
20	18	0	5.30	0.00

C, LEU				
Chromosome	Number of events		Mbp-cl	
	Gain	Loss	Gain	Loss
14	4	4	1.77	2.44

TUM, tumor tissue; ADJ, adjacent non-tumor tissue; LEU, leukocytes; Mbp, mega-base pairs; cl, cumulative length.

organism based on the CNV genes associated with Hallmarks of Cancer (Table V). In TUM, the most significantly enriched pathways included 'DNA repair' (NER and TP53 signaling), 'extracellular matrix remodeling' (collagen assembly) and 'cell cycle checkpoints' (G2/M). In ADJ, enrichment was observed in 'NOTCH signaling' and 'RAC3 GTPase cycle' pathways, while LEU showed limited enrichment, with IGLL5 associated with 'antigen binding' and 'immune activation'.

*Interaction gene networks.* CNV genes associated with Hallmarks of Cancer and linked to metabolic pathways were used to construct interaction networks using STRING (Fig. 3). Edges represent associations based on metabolic pathways, gene expression, localization, inferred interactions, genetic interactions, data mining and neighborhood associations. Each node was annotated with flags corresponding to the reported hallmarks. In the LEU network, a single node representing IGLL5 was observed. In ADJ, the genes with the highest number of connections were E1A-binding protein p300 and RECQL4. The TUM network contained 39 nodes, with ERCC4, EGFR and HSP90AB1 showing the highest connectivity. Notably, EGFR, telomerase reverse transcriptase, neurotrophic receptor tyrosine kinase 1 and ribosomal protein S6 kinase B1 were associated with the largest number of hallmarks within the network (Table VI) (39,49,53-64).

Table IV. Cytobands and chromosomes affected by CNV cumulative length.

A, Tumor tissue				
Chromosome	Cytoband	Length, Mbp-cl	Type	Number of patients
1	q23.3	12.77	Gain	5
1	q32.1	7.03	Gain	5
6	q25.2	3.18	Loss	5
8	q24.22	20.32	Gain	5
8	q24.3	16.25	Gain	5

B, Adjacent non-tumor tissue				
Chromosome	Cytoband	Length, Mbp-cl	Type	Number of patients
1	p36.32	3.61	Gain	5
4	p16.1	3.84	Gain	5
5	p15.33	5.15	Gain	4
8	q24.3	9.03	Gain	5
20	q13.33	4.98	Gain	5

C, Leukocytes				
Chromosome	Cytoband	Length, Mbp-cl	Type	Number of patients
8	p11.22	0.47	Loss	3
14	q11.2	1.77	Loss	4
14	q32.33	2.44	Gain	4
22	q11.22	0.77	Gain	3

Mbp-cl, mega-base pairs-cumulative length.

## Discussion

To the best of our knowledge, the present study is among the first genome-wide high-density CNV analyses of TNBC in Mexican patients using matched sample sets comprising TUM, ADJ and LEU. The results revealed a complex landscape of genomic alterations involving both shared and unique CNVs across these sample types. The present findings highlight the value of CNVs not only in tumorigenesis but also in the tumor microenvironment and peripheral blood, suggesting a broader systemic genomic instability.

Genomic studies in Latin American populations have identified founder mutations and distinct variant distributions in BC susceptibility genes (34-36), highlighting genuine population-level genetic diversity. However, the present small sample size and single-center design limit the ability to distinguish population-specific patterns from sampling variability or technical factors. Larger, multi-center studies are needed to validate whether the CNV patterns in the present study represent true population-specific signatures or reflect individual tumor heterogeneity.

Chromosomal regions such as 1q23.3, 1q32.1 and 8q24.3 showed consistent gains across tumor samples. These loci harbor oncogenes such as MCL1, BCL9 and MYC, which are

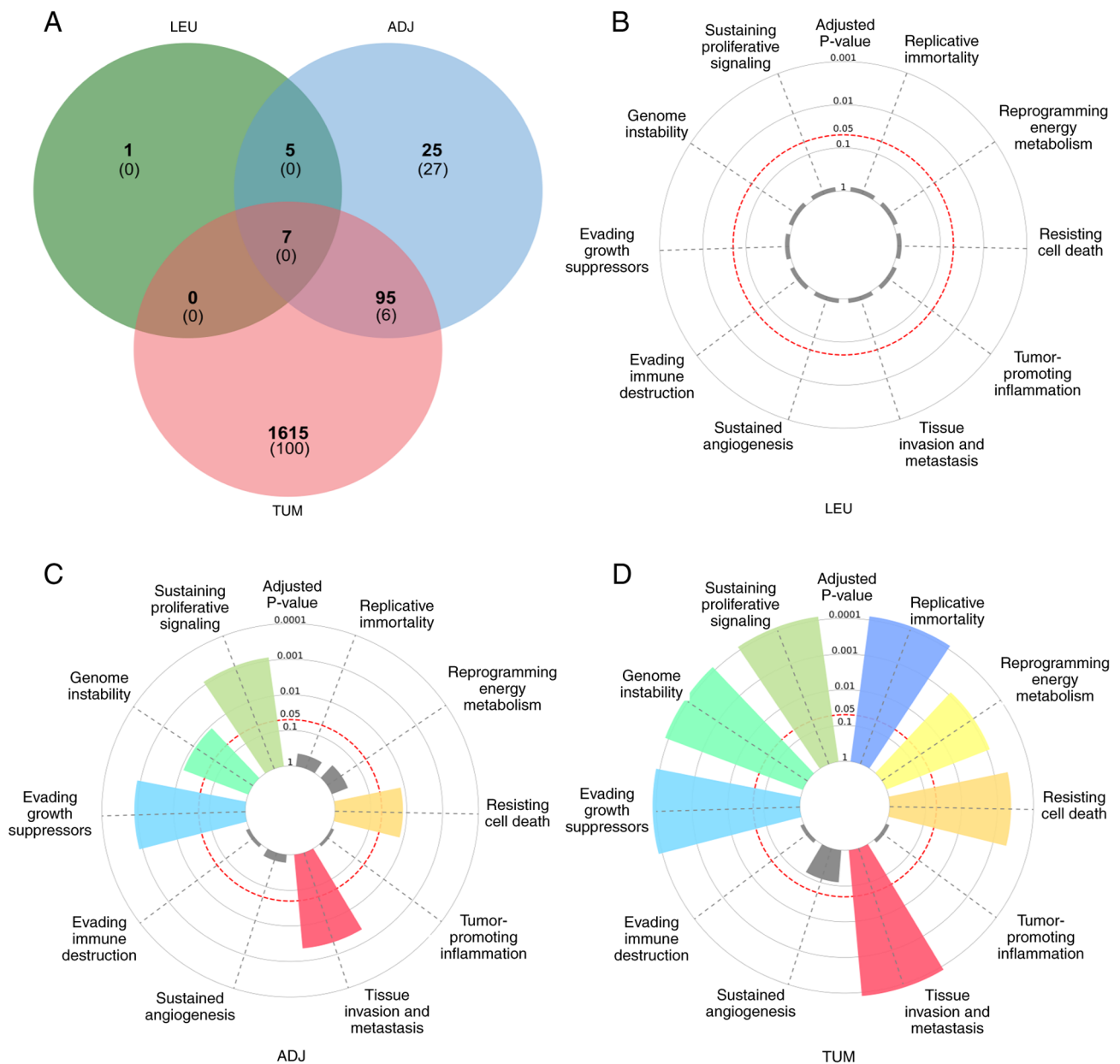


Figure 2. Hallmark of Cancer enrichment plot. Profile of CNV-genes in triple negative breast cancer from  $\geq 3$  patients showing frequency of unique and shared CNV-affected genes. (A) Frequency of unique and shared CNV-affected genes in  $\geq 3$  patients across TUM, ADJ and LEU. Numbers in brackets indicate the count of CNV-affected genes for each region of the Venn diagram. (B) LEU, (C) ADJ and (D) TUM. CNV, copy number variation; TUM, tumor tissue; ADJ, adjacent non-tumor tissue; LEU, leukocytes.

implicated in cancer progression, resistance to apoptosis and metastasis (29,30,37). Gains in 8q24.3 and 20q13.33 are associated with amplification of MYC and ZNF217, respectively, which promote tumor proliferation and metastasis (29,30). Gains on chromosome 1q are established markers of poor prognosis in BC (29,30,38). By contrast, losses in 6q25.2, encompassing the ESR1 gene, are aligned with hormone receptor-negative phenotypes, reinforcing the clinical characteristics of TNBC (29,30,33). Furthermore, gains in 20q13.33 (ZNF217) and 8q24.3 were also detected in ADJ and LEU, supporting the hypothesis that CNVs may originate early in tumorigenesis or reflect systemic alterations.

Hallmarks of Cancer enrichment analysis confirmed that TUM samples predominantly showed CNVs associated with processes such as proliferation, invasion, metastasis and

immune evasion, while ADJ samples were associated with growth suppression and LEU samples with genomic instability. This stratification underlines the molecular heterogeneity of TNBC and offers a nuanced view of how genomic alterations influence tumor behavior and the microenvironment.

Functional pathway analysis further validated these findings. In TUM, pathways associated with DNA repair (NER and TP53 signaling), extracellular matrix remodeling (collagen assembly) and cell cycle checkpoints (G2/M) were significantly enriched. These molecular disruptions are consistent with the TNBC aggressive phenotype and poor response to conventional therapy. ADJ showed enrichment in NOTCH and RAC3 signaling, suggesting that non-malignant cells within the tumor microenvironment may also undergo functional reprogramming, potentially contributing to tumor support or resistance mechanisms.

Table V. Metabolic pathways and genes of the Hallmarks of Cancer.

A, Tumor tissue			
Pathway category	Reactome process	P-value	Genes
DNA repair	Dual incision in TC-NER and GG-NER, TP53 regulates transcription	<0.001	CDK7, ERCC4, UVSSA, POLE2, POLD2, GTF2H2, ERCC6, CDK12
Extracellular matrix/collagen	Laminin interactions, assembly of collagen fibrils, and collagen degradation	<0.001	COL4A1, COL4A2, ITGA3, LAMB3, PRSS2
Cell signaling	TRKA receptor activation and downstream RAS/ERK/MAPK and PI3K signaling cascades	0.008	ALK, EGFR, NTRK1, PIK3CB, RALA, ADCYAP1R1, NRG2
Cell cycle and checkpoints	G2/M checkpoints, DNA replication checkpoint, BRCA2, ATR	0.021	CCNB1, CCNB2, HUS1, RAD17
Regulation by TP53	Formation of the early elongation complex, transcription of death receptors and ligands	0.036	CDK12, CDK7, IGFBP3, PMS2
Development and diseases	Chondrocyte maturation, defective LFNG causes SCDO3, disorders of developmental biology	0.029	GLI2, HDAC4, NCOR2, NOTCH1, TBL1XR1
Cellular stress response	HSF1-dependent transactivation, attenuation phase	0.001	HSF1, CAMK2B, HSP90AB1, HSPA6
B, Adjacent non-tumor tissue			
Signal transduction	Signaling NOTCH2, RAC3 GTPase cycle	0.002	EP300, HES5, ARHGAP39, BAIAP2
Neuronal system	Sodium-permeable postsynaptic acetylcholine nicotinic receptors	0.020	CHRNA4
Metabolism	Alanine metabolism	0.020	GPT
Developmental biology	MITF-M-dependent genes involved in DNA replication, damage repair and senescence, transcriptional factor binding	0.023	TERT, SOX8, EP300, BAIAP2, TP73, PRDM16
Immune system	Co-inhibition by BTLA	0.033	TNFRSF14
C, Leukocytes			
Metabolism and Antigen binding	Biological oxidations B-cell activation	0.012 0.036	IGLL5

The present study identified a subset of CNV genes with high network centrality and multiple hallmark associations, such as EGFR, ERCC4 and HSP90AB1, suggesting potential as markers or therapeutic targets. EGFR was highly connected within the network and amplified in several patients, consistent with its role in TNBC and previous reports of upregulation in Latin American cohorts (39).

However, there are limitations of network-based analyses. STRING (25) and GeneMANIA databases compile information from diverse sources, including protein-protein interactions, co-expression patterns and pathway annotations. Consequently, genes such as EGFR and HSP90AB1, which are extensively studied and participate in multiple cell processes (40,41), inherently exhibit higher node connectivity regardless of specific CNV data. This bias may influence

their classification as core nodes and should be interpreted with caution. The high centrality of these genes in the present networks reflects both their biological relevance to cancer and their extensive characterization in existing databases.

The LEU network, comprising only IGLL5, demonstrated limited biological significance for network topology analysis. IGLL5 has been reported as upregulated in immune signatures associated with relapse-free survival in patients with BC (42). Future studies with larger cohorts may reveal additional CNV-affected genes in peripheral blood, enabling more robust network analyses.

Genomic studies typically underrepresent Latin American populations, leading to limited generalizability of findings and complicating clinical interpretation (35,36). The present results emphasize the importance of population-specific genomic

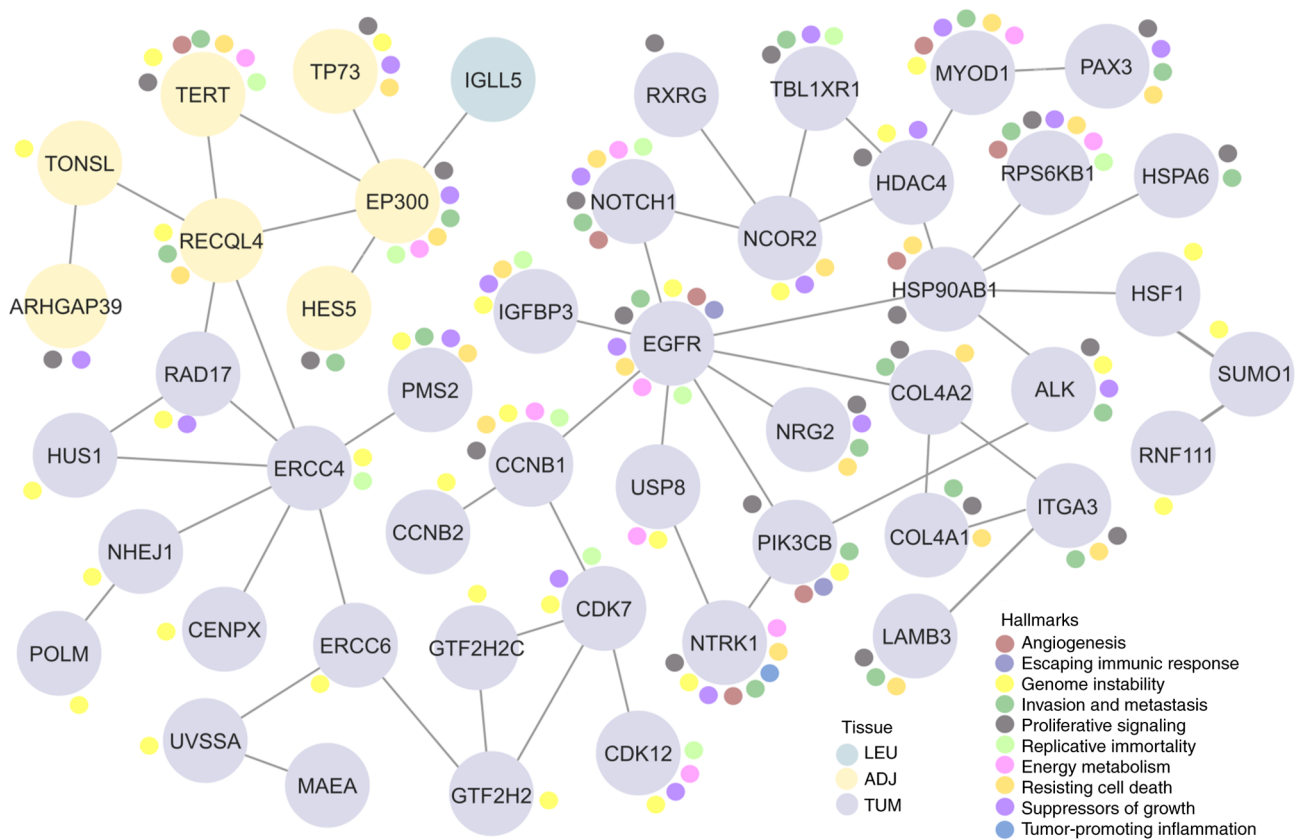


Figure 3. Gene interaction networks associated with Hallmarks of Cancer and metabolic pathways in CNV-affected genes in triple-negative breast cancer. TUM, tumor tissue; ADJ, adjacent non-tumor tissue; LEU, leukocytes.

studies to uncover potentially unique molecular signatures that may inform diagnosis, prognosis or therapy in these groups.

Finally, although the present results provide valuable insight, several limitations should be acknowledged. The small sample size restricted statistical power, and the absence of RNA expression data prevented functional validation of the identified CNVs. Of ~400 BC samples assessed for inclusion, only those containing  $\geq 70\%$  cancer cells were included. This threshold was established as a quality criterion to minimize signal noise introduced by non-cancerous cells, thereby ensuring the reliability of CNV detection in tumor samples (43,44). Histological assessment of the biopsies was performed by two trained pathologists independently. They assigned the phenotypic diagnosis of TNBC. Only samples with the same diagnosis (identical results) by two independent expert pathologists were included in the analysis.

Nonetheless, the integration of CNV profiles with hallmark functions and interaction networks presents a robust framework for understanding TNBC heterogeneity and identifying candidate molecular targets. The CNV frequencies are important for data filtering and analysis.

Including populations from diverse ethnic backgrounds in genomic analyses is key for ensuring that reference databases, variant interpretation tools and clinical guidelines are applicable across demographic groups. Without adequate representation, genetic test results from individuals with non-European backgrounds are difficult to interpret, limiting both the clinical utility and the equitable delivery of genetic testing (34).

Computational and experimental approaches, including NGS-based algorithms, SNP array analyses and bioinformatics pipelines, have been developed to detect CNVs as crucial markers for tumors, with potential implications in tumor subtyping and predicting responses to therapy (43,45). However, reliable CNV detection can be hindered by challenges such as normal cell contamination, tumor heterogeneity and systematic errors resulting from structural variations (43,46). Therefore, it is recommended to identify these variations before conducting CNV analysis on tumor samples.

Recent advances in CNV analysis have established robust frameworks for integrating data from diverse platforms (47,48). Steele *et al* (49) developed a pan-cancer CN signature framework applicable to whole-genome and exome sequencing and SNP microarray data, identifying 21 signatures across 9,873 cancer cases from TCGA. The framework demonstrated that BC, along with ovarian cancer, overrepresents CNVs relative to other genomic alterations. A subsequent study (50) expanded on these findings by analyzing whole-genome sequencing and SNP array data from TCGA. This work validated 14 CNV signatures and established the prognostic relevance of specific signature activities across multiple cancer types.

For TNBC, integrative network-based approaches have proven valuable for identifying key driver genes and therapeutic targets. Singh *et al* (51) employed protein-protein interaction network analysis combined with weighted gene co-expression network analysis to identify 13 key genes in

Table VI. Genes linked to the highest number of Hallmarks of Cancer and genes detected in breast cancer.

A, Tumor tissue			
Gene	Chromosome and cytoband	Alteration in triple-negative breast cancer	(Refs.)
EGFR	7p11.2	Amplification in ~14% breast tumors, including Mexican cases, functions in cellular processes	(39)
ERCC4	16p13.12	Moderate-level CNAs (amplifications/deletions) involving ERCC4 in metastatic breast cancer. DNA repair processes that remove damage and maintain chromosome stability are generated by the proteins encoded by the ERCC genes	(53)
HSP90AB1	6p21.1	Promotes tumor-associated macrophage differentiation	(54)
NOTCH1	9q34.3	Upregulated in triple-negative breast cancer in Latin American female patients; linked to lower overall survival	(55)
NTRK1	1q23.1	Copy number gain and amplification are frequent events, suggesting a possible predictive role for other NTRK aberrations	(56)
COL4A2	13q34	Upregulation of COL4A2 at 13q34 enhances cell migration and proliferation	(57)
CCNB1	5q13.2	Aberrant levels of the G2/M cyclin B1 (gene CCNB1) are associated with multiple types of cancer; it is a key player in breast cancer progression and potential biomarkers for prognosis. Furthermore, their roles in immune regulation suggest they may be promising targets for immunotherapy	(58) (59)
IGFBP3	7p12.3	IGFBP-3 negatively regulates MCF-7 breast cancer cell proliferation by inducing senescence via telomerase suppression	(60)
B, Adjacent non-tumor tissue			
EP300	22q13.2	Epigenome control and chromatin remodeling enzymes	(61)
TERT	5p15.33	Expression was significantly correlated with immune cell infiltration, common immunomodulators	(62)
ARHGAP39	8q13.1	Upregulated; prognostic biomarker tied to immune infiltration based on The Cancer Genome Atlas and Clinical Proteomic Tumor Analysis Consortium database and validated by quantitative PCR	(63)
TP73	p36.32	High expression, aberrant methylation	(64)
C, Leukocytes			
IGLL5	22q11.22	Upregulated in the immune signature linked to predictor of relapse-free survival	(59)

TNBC, including EGFR, demonstrating the utility of network topology for biomarker discovery. The present study extended these methodological advances by employing high-resolution Affymetrix CytoScan HD arrays with stringent quality control (MAPD <0.25), analyzing CNVs in TUM, ADJ and LEU to distinguish somatic from potential germline alterations, integrating CNV data with Hallmarks of Cancer enrichment analysis and constructing interaction networks to identify central nodes. To the best of our knowledge, the present study is the first multi-layered CNV analytical framework applied to TNBC samples from Mexican patients, addressing a critical gap in genomic diversity research.

The present study demonstrated the value of integrating high-density CNV profiling with network-based analyses of TUM, ADJ and blood samples. This approach offers a systemic view of genomic instability in TNBC and identifies recurrent alterations and central nodes in cancer-associated pathways, while also contributing to the representation of Latin American populations in genomic research (35,36). The present methodological framework can be extended to other cohorts and cancer subtypes, facilitating the transition from descriptive variation maps to functionally relevant biomarkers. Notably, population-specific genomic references provide a basis for the development of equitable precision oncology

strategies and collaborations that address global disparities in cancer research and care (35,36,52).

### Acknowledgements

The authors would like to thank Ms Irma P. Ramos-Vega, Infectious and Parasitic Diseases Medical Research Unit, High Specialty Medical Unit (UMAE)-Pediatrics Hospital 'Dr. Silvestre Frenk Freund', XXI Century National Medical Center, Mexico City, Mexico; Mexican Social Security Institute (IMSS), Mexico City, Mexico. Mr. Brian-Alexander Cruz-Ramírez and Ms. Araceli Peralta-Aguilar, Oncological Diseases Medical Research Unit, UMAE-Oncology Hospital, XXI Century National Medical Center, IMSS, Mexico City, Mexico, for their technical assistance.

### Funding

The present study was supported by the Fondo de Investigación en Salud-Instituto Mexicano del Seguro Social (grant nos. FIS/IMSS/PROT/PRI0/13/027 and R-2020-785-154).

### Availability of data and materials

The data generated in the present study may be found in the Gene Expression Omnibus under accession number GSE290707 or at the following URL: [www.ncbi.nlm.nih.gov/geo/query/acc.cgi?acc=GSE290707](http://www.ncbi.nlm.nih.gov/geo/query/acc.cgi?acc=GSE290707).

### Authors' contributions

VLS, HAVS and MERT performed the experiments, analyzed data and wrote the manuscript. JT, MCP, PPS and HM supervised biological sample collection, interpreted data and revised the manuscript. MERT designed and supervised the study and revised the manuscript. VLS, HAVS and MERT confirm the authenticity of all the raw data. All authors have read and approved the final manuscript.

### Ethics approval and consent to participate

National Commission for Scientific Research of the Health Research Coordination (CIS) of the Mexican Social Security Institute (IMSS, Mexico City, Mexico) approval was obtained for the study (approval no. 2008-785-001). Clinical data and patient samples were processed following written informed consent.

### Patient consent for publication

Not applicable.

### Competing interests

The authors declare that they have no competing interests.

### Use of artificial intelligence

During the preparation of this work, artificial intelligence tools were used to improve the readability and language

(Grammarly) of the manuscript, and subsequently, the authors revised and edited the content produced by the artificial intelligence tools as necessary, taking full responsibility for the ultimate content of the present manuscript.

### References

1. International Agency for Research on Cancer (IARC): Global Cancer Observatory: Cancer Today. Lyon, France: IARC. Available from: <https://gco.iarc.who.int/today>. Accessed September 6, 2025.
2. Hanahan D and Weinberg RA: Hallmarks of cancer: The next generation. *Cell* 144: 646-674, 2011.
3. Plowman JN, Matoy EJ, Uppala LV, Draves SB, Watson CJ, Sefranek BA, Stacey ML, Anderson SP, Belshan MA, Blue EE, *et al*: Targeted sequencing for hereditary breast and ovarian cancer in BRCA1/2-negative families reveals complex genetic architecture and phenocopies. *HGG Adv* 5: 100306, 2024.
4. Patel MM and Adrada BE: Hereditary breast cancer: BRCA mutations and beyond. *Radiol Clin North Am* 62: 627-642, 2024.
5. Pal M, Das D and Pandey M: Understanding genetic variations associated with familial breast cancer. *World J Surg Oncol* 22: 271, 2024.
6. Reiner AS, Watt GP, Malone KE, Lynch CF, John EM, Knight JA, Woods M, Liang X, Tischkowitz M, Conti DV, *et al*: Breast cancer susceptibility gene sequence variations and development of contralateral breast cancer. *JAMA Netw Open* 7: e2452158, 2024.
7. Krepischi AC, Achatz MIW, Santos EM, Costa SS, Lisboa BC, Brentani H, Santos TM, Gonçalves A, Nóbrega AF, Pearson PL, *et al*: Germline DNA copy number variation in familial and early-onset breast cancer. *Breast Cancer Res* 14: R24, 2012.
8. Dennis J, Tyrer JP, Walker LC, Michailidou K, Dorling L, Bolla MK, Wang Q, Ahearn TU, Andrulis IL, Anton-Culver H, *et al*: Rare germline copy number variants (CNVs) and breast cancer risk. *Commun Biol* 5: 65, 2022.
9. Hernández-Gómez C, Hernández-Lemus E and Espinal-Enríquez J: The role of copy number variants in gene co-expression patterns for luminal B breast tumors. *Front Genet* 13: 806607, 2022.
10. Pylkäs K, Vuorela M, Otsukka M, Kallioniemi A, Jukkola-Vuorinen A and Winqvist R: Rare copy number variants observed in hereditary breast cancer cases disrupt genes in estrogen signaling and TP53 tumor suppression network. *PLoS Genet* 8: e1002734, 2012.
11. Kumpula TA, Vorimo S, Mattila TT, O'Gorman L, Astuti G, Tervasmäki A, Koivuluoma S, Mattila TM, Grip M, Winqvist R, *et al*: Exome sequencing identified rare recurrent copy number variants and hereditary breast cancer susceptibility. *PLoS Genet* 19: e1010889, 2023.
12. Zavala VA, Serrano-Gomez SJ, Dutil J and Fejerman L: Genetic epidemiology of breast cancer in Latin America. *Genes (Basel)* 10: 153, 2019.
13. Larios-Serrato V, Martínez-Ezquerro JD, Valdez-Salazar HA, Torres J, Camorlinga-Ponce M, Piña-Sánchez P and Ruiz-Tachiquín ME: Copy number alterations and epithelial-mesenchymal transition genes in diffuse and intestinal gastric cancers in Mexican patients. *Mol Med Rep* 25: 191, 2022.
14. Utrera-Barillas D, Valdez-Salazar HA, Gómez-Rangel D, Alvarado-Cabrero I, Aguilera P, Gómez-Delgado A and Ruiz-Tachiquín ME: Is human cytomegalovirus associated with breast cancer progression? *Infect Agent Cancer* 8: 12, 2013.
15. Haraksingh RR, Abyzov A and Urban AE: Comprehensive performance comparison of high-resolution array platforms for genome-wide copy number variation (CNV) analysis in humans. *BMC Genomics* 18: 321, 2017.
16. Wang K, Li M, Hadley D, Liu R, Glessner J, Grant SF, Hakonarson H and Bucan M: PennCNV: An integrated hidden Markov model designed for high-resolution copy number variation detection in whole-genome SNP genotyping data. *Genome Res* 17: 1665-1674, 2007.
17. McKusick-Nathans Institute of Genetic Medicine, Johns Hopkins University: Online Mendelian Inheritance in Man, OMIM®. <https://omim.org>. Accessed January 2024.

18. Firth HV, Richards SM, Bevan AP, Clayton S, Corpas M, Rajan D, Van Vooren S, Moreau Y, Pettett RM and Carter NP: DECIPHER: Database of chromosomal imbalance and phenotype in humans using ensembl resources. *Am J Hum Genet* 84: 524-533, 2009.
19. Zhao M, Liu Y, Zheng C and Qu H: dbEMT 2.0: An updated database for epithelial-mesenchymal transition genes with experimentally verified information and precalculated regulation information for cancer metastasis. *J Genet Genomics* 46: 595-597, 2019.
20. Gel B and Serra E: karyoploteR: An R/bioconductor package to plot customizable genomes displaying arbitrary data. *Bioinformatics* 33: 3088-3090, 2017.
21. Durinck S, Spellman PT, Birney E and Huber W: Mapping identifiers for the integration of genomic datasets with the R/bioconductor package biomaRt. *Nat Protoc* 4: 1184-1191, 2009.
22. Bardou P, Mariette J, Escudié F, Djemiel C and Klopp C: jvenn: An interactive Venn diagram viewer. *BMC Bioinformatics* 15: 293, 2014.
23. Menyhart O, Kothalawala WJ and Györfy B: A gene set enrichment analysis for cancer hallmarks. *J Pharm Anal* 15: 101065, 2025.
24. Fabregat A, Jupe S, Matthews L, Sidiropoulos K, Gillespie M, Garapati P, Haw R, Jassal B, Korninger F, May B, *et al*: The reactome pathway knowledgebase. *Nucleic Acids Res* 46 (D1): D649-D655, 2018.
25. Szklarczyk D, Kirsch R, Koutrouli M, Nastou K, Mehryary F, Hachilif R, Gable AL, Fang T, Doncheva NT, Pyysalo S, *et al*: The STRING database in 2023: Protein-protein association networks and functional enrichment analyses for any sequenced genome of interest. *Nucleic Acids Res* 51 (D1): D638-D646, 2023.
26. Warde-Farley D, Donaldson SL, Comes O, Zuberi K, Badrawi R, Chao P, Franz M, Grouios C, Kazi F, Lopes CT, *et al*: The GeneMANIA prediction server: Biological network integration for gene prioritization and predicting gene function. *Nucleic Acids Res* 38 (Web Server Issue): W214-W220, 2010.
27. Shannon P, Markiel A, Ozier O, Baliga NS, Wang JT, Ramage D, Amin N, Schwikowski B and Ideker T: Cytoscape: A software environment for integrated models of biomolecular interaction networks. *Genome Res* 13: 2498-2504, 2003.
28. Uhlen M, Zhang C, Lee S, Sjöstedt E, Fagerberg L, Bidkhori G, Benfèitas R, Arif M, Liu Z, Edfors F, *et al*: A pathology atlas of the human cancer transcriptome. *Science* 357: eaan2507, 2017.
29. Curtis C, Shah SP, Chin SF, Turashvili G, Rueda OM, Dunning MJ, Speed D, Lynch AG, Samarajiwa S, Yuan Y, *et al*: The genomic and transcriptomic architecture of 2,000 breast tumours reveals novel subgroups. *Nature* 486: 346-352, 2012.
30. Cancer Genome Atlas Network: Comprehensive molecular portraits of human breast tumours. *Nature* 490: 61-70, 2012.
31. Yu G and He QY: ReactomePA: An R/bioconductor package for reactome pathway analysis and visualization. *Mol Biosyst* 12: 477-479, 2016.
32. Wickham H: ggplot2: Elegant graphics for data analysis. Springer-Verlag, New York, 2016.
33. Derakhshan F and Reis-Filho JS: Pathogenesis of triple-negative breast cancer. *Annu Rev Pathol* 17: 181-204, 2022.
34. Fernández-Lopez JC, Romero-Córdoba S, Rebollar-Vega R, Alfaro-Ruiz LA, Jiménez-Morales S, Beltrán-Anaya F, Arellano-Llamas R, Cedro-Tanda A, Rios-Romero M, Ramírez-Florencio M, *et al*: Population and breast cancer patients' analysis reveals the diversity of genomic variation of the BRCA genes in the Mexican population. *Hum Genomics* 13: 3, 2019.
35. Borda V, Loesch DP, Guo B, Laboulaye R, Veliz-Otani D, French JN, Leal TP, Gogarten SM, Ikpe S, Gouveia MH, *et al*: Genetics of Latin American diversity project: Insights into population genetics and association studies in admixed groups in the Americas. *Cell Genom* 4: 100692, 2024.
36. Ruíz-Patiño A, Rojas L, Zuluaga J, Arrieta O, Corrales L, Martín C, Franco S, Raelz L, Rolfo C, Sánchez N and Cardona AF: Genomic ancestry and cancer among Latin Americans. *Clin Transl Oncol* 26: 1856-1871, 2024.
37. Vafaizadeh V, Buechel D, Rubinstein N, Kalathur RKR, Bazzani L, Saxena M, Valenta T, Hausmann G, Cantù C, Basler K and Christofori G: The interactions of Bcl9/Bcl9L with  $\beta$ -catenin and Pygopus promote breast cancer growth, invasion, and metastasis. *Oncogene* 40: 6195-6209, 2021.
38. Shahrouzi P, Forouz F, Mathelier A, Kristensen VN and Duijf PHG: Copy number alterations: A catastrophic orchestration of the breast cancer genome. *Trends Mol Med* 30: 750-764, 2024.
39. Connor AE, Baumgartner RN, Baumgartner KB, Pinkston CM, John EM, Torres-Mejía G, Hines LM, Giuliano AR, Wolff RK and Slattery ML: Epidermal growth factor receptor (EGFR) polymorphisms and breast cancer among Hispanic and non-Hispanic white women: The breast cancer health disparities study. *Int J Mol Epidemiol Genet* 4: 235-249, 2013.
40. Albakova Z, Mangasarova Y, Albakov A and Gorenkova L: HSP70 and HSP90 in cancer: cytosolic, endoplasmic reticulum and mitochondrial chaperones of tumorigenesis. *Front Oncol* 12: 829520, 2022.
41. Albakova Z: HSP90 multi-functionality in cancer. *Front Immunol* 15: 1436973, 2024.
42. Shi H, Bevier M, Johansson R, Enquist-Olsson K, Henriksson R, Hemminki K, Lenner P and Försti A: Prognostic impact of polymorphisms in the MYBL2 interacting genes in breast cancer. *Breast Cancer Res Treat* 131: 1039-1047, 2012.
43. Masood D, Ren L, Nguyen C, Brundu FG, Zheng L, Zhao Y, Jaeger E, Li Y, Cha SW, Halpern A, *et al*: Evaluation of somatic copy number variation detection by NGS technologies and bioinformatics tools on a hyper-diploid cancer genome. *Genome Biol* 25: 163, 2024.
44. Chandramohan R, Reuther J, Gandhi I, Voicu H, Alvarez KR, Plon SE, Lopez-Terrada DH, Fisher KE, Parsons DW and Roy A: A validation framework for somatic copy number detection in targeted sequencing panels. *J Mol Diagn* 24: 760-774, 2022.
45. Du R, Dong J, Jiang H, Qi M and Zhao Z: Comparative study of tools for copy number variation detection using next-generation sequencing data. *Sci Rep* 15: 22145, 2025.
46. Oketch DJA, Giulietti M and Piva F: Copy number variations in pancreatic cancer: From biological significance to clinical utility. *Int J Mol Sci* 25: 391, 2023.
47. Hazra A, O'Hara A, Polyak K, Nakhlis F, Harrison BT, Giordano A, Overmoyer B and Lynce F: Copy number variation in inflammatory breast cancer. *Cells* 12: 1086, 2023.
48. Yan K, Niu L, Wu B, He C, Deng L, Chen C, Lan Z, Lin C, Kuang W, Lin H, *et al*: Copy number variants landscape of multiple cancers and clinical applications based on NGS gene panel. *Ann Med* 55: 2280708, 2023.
49. Steele CD, Abbasi A, Islam SMA, Bowes AL, Valber A, Khandekar A, Pickering L, Boyle JM, East P, Pearson A, *et al*: Signatures of copy number alterations in human cancer. *Nature* 606: 984-991, 2022.
50. Tao Z, Wang S, Wu C, Wu T, Zhao X, Ning W, Wang G, Wang J, Chen J, Diao K, *et al*: The repertoire of copy number alteration signatures in human cancer. *Brief Bioinform* 24: bbad053, 2023.
51. Singh P, Chaturvedi R and Somvanshi P: Network-based integrative analysis to identify key genes and corresponding reporter biomolecules for triple-negative breast cancer. *Cancer Med* 14: e70674, 2025.
52. Cheung ATM, Palapattu EL, Pompa IR, Aldrighetti CM, Niemierko A, Willers H, Huang F, Vapiwala N, Van Allen E and Kamran SC: Racial and ethnic disparities in a real-world precision oncology data registry. *NPJ Precis Oncol* 7: 7, 2023.
53. Hermawan A and Putri H: Characterizing excision repair cross-complementing family genes as drug resistance biomarkers in breast cancer. *Beni Suef Univ J Basic Appl Sci* 12: 79, 2023.
54. Hong L, Tanaka M, Yasui M and Hara-Chikuma M: HSP90 promotes tumor associated macrophage differentiation during triple-negative breast cancer progression. *Sci Rep* 14: 22541, 2024.
55. Gómez-Archila JD, Espinosa-García AM, Palacios-Reyes C, Trujillo-Cabrera Y, Mejía ALS, González AVA, Rangel-López E, Alonso-Themann PG, Solís NDS, Hernández-Zavala A, *et al*: NOTCH expression variability and relapse of breast cancer in high-risk groups. *Am J Med Sci* 364: 583-594, 2022.
56. Zito Marino F, Buono S, Montella M, Giannatiempo R, Messina F, Casaretta G, Arpino G, Vita G, Fiorentino F, Insabato L, *et al*: NTRK gene aberrations in triple-negative breast cancer: Detection challenges using IHC, FISH, RT-PCR, and NGS. *J Pathol Clin Res* 9: 367-377, 2023.

57. Li X, Jin Y and Xue J: Unveiling Collagen's role in breast cancer: Insights into expression patterns, functions and clinical implications. *Int J Gen Med* 17: 1773-1787, 2024.
58. Dai P, Xiong L, Wei Y, Wei X, Zhou X, Zhao J and Tang H: A pancancer analysis of the oncogenic role of cyclin B1 (CCNB1) in human tumors. *Sci Rep* 13: 16226, 2023.
59. Su Q, Fang L, Li C, Yue L, Yun Z, Zhang H, Liu Q, Ma R, Zhong P, Liu H, *et al*: Multi-omics insights into the roles of CCNB1, PLK1, and HPSE in breast cancer progression: Implications for prognosis and immunotherapy. *Discov Oncol* 16: 471, 2025.
60. Kwon A, Chae HW, Lee WJ, Kim J, Kim YJ, Ahn J, Oh Y and Kim HS: Insulin-like growth factor binding protein-3 induces senescence by inhibiting telomerase activity in MCF-7 breast cancer cells. *Sci Rep* 13: 8739, 2023.
61. Gronkowska K and Robaszkiewicz A: Genetic dysregulation of EP300 in cancers in light of cancer epigenome control-targeting of p300-proficient and -deficient cancers. *Mol Ther Oncol* 32: 200871, 2024.
62. Lin F, Huang J, Zhu W, Jiang T, Guo J, Xia W, Chen M, Guo L, Deng W and Lin H: Prognostic value and immune landscapes of TERT promoter methylation in triple negative breast cancer. *Front Immunol* 14: 1218987, 2023.
63. Yao L, Li Y, Li S, Wang M, Cao H, Xu L and Xu Y: ARHGAP39 is a prognostic biomarker involved in immune infiltration in breast cancer. *BMC Cancer* 23: 440, 2023.
64. Gomez LC, Sottile ML, Guerrero-Gimenez ME, Zoppino FCM, Redondo AL, Gago FE, Orozco JI, Tello OM, Roqué M, Nadin SB, *et al*: TP73 DNA methylation and upregulation of  $\Delta$ Np73 are associated with an adverse prognosis in breast cancer. *J Clin Pathol* 71: 52-58, 2018.



Copyright © 2026 Larios-Serrato et al. This work is licensed under a Creative Commons Attribution-NonCommercial 4.0 International (CC BY-NC 4.0) License.